J Therm Anal Calorim (2012) 107:869–875
DOI 10.1007/s10973-011-1567-9

# Synthesis, spectroscopic and thermal properties of Pt(II) complexes of some polydentate ligands

**Yakup Baran · Ismet Kaya · Murat Turkyılmaz**

Received: 23 February 2011 / Accepted: 5 April 2011 / Published online: 21 April 2011


**Abstract** The new tetradentate symmetrical (2*R*,2′S)-1,1′-piperazine-1,4-diyldipropane-2-thiol) ($L^1$), (2*S*)-1-[bis(2-aminoethyl)amino]propan-2-ol) ($L^2$), and 2-{(*E*)-[((1*R*,2*S*)-2-{[(1*Z*)-(2-hydroxy phenyl)methylene]amino}cyclohexyl)imino]methyl}phenol ($L^3$) ligands were synthesized and characterized on the basis of FT-IR, $^1$H, $^{13}$C NMR, EI mass, and elemental analysis. Three commercially available ligands, (2,2′-[ethane-1,2-diylbis(thio)]diethanol ($L^4$), 2,2′-dithiodiethanenamine ($L^5$), and (2,2′-[ethane-1,2-diyldi(imino)] diethanol ($L^6$), were also studied. Pt(II) complexes were characterized by FTIR, elemental analysis and thermal methods. Thermal behaviors of these complexes were investigated in the range 10–1000 °C. Magnetic properties were also studied, and the all complexes were found to be diamagnetic. The structures consist of the monomeric units in which the Pt(II) atoms exhibit square planar geometry. *N,N′*-bis(salicylidene)-1,2-cyclohexane has been synthesized and characterized by X-ray single crystal diffraction measurement. The ligand crystallizes in monoclinic crystal system and space group, Cc.

**Keywords** Pt(II) · Polydentate · FTIR · TG · NMR · Thermal stability · X-ray

Y. Baran (✉) · I. Kaya
Department of Chemistry, Art and Science Faculty, Onsekiz Mart University, Canakkale 17100, Turkey
e-mail: yakupbaran@yahoo.com

M. Turkyılmaz
Department of Chemistry, Science Faculty, Trakya University, Edirne, Turkey

## Introduction

Due to their importance in coordination chemistry, complexes of tetra-coordinated ligands and transition metals are extensively studied. These complexes present many applications in catalysis and oxygen storage devices [1]. Most of them show antiviral and antibacterial activity [2] and also used as mimic system for enzyme models [3]. Acyclic polydentate ligands are important member of chelating ligands which were used in coordination chemistry for their metal binding ability. Transition metals are essential metallic elements and exhibit great biological activity when associated with certain metal–protein complexes, participating in oxygen transport, electronic transfer reactions, or storage of ions [4]. Since the discovery of *cis*-platin as cancerostatic compounds and the successful clinical application of these compounds, the investigation of related platinium complexes has been widespread interest. *Cis*-platin is still one of the most widely used drugs in chemotherapy, while its side effect is important. The high stability potential of the Pt(II) complexes with tetradentate ligands extended the application of these compounds in a wide range. As a tetradentate ligands, some Schiff base–metal complexes are characterized by interesting and important properties such as biological activity [5–7], catalytic activity [8], and photochromic properties [9, 10]. Tetradentate Schiff bases containing nitrogen and oxygen donor atoms such as *N,N′*-bis(salicylidene)-1,2-cyclohexanediamine. $L^3$ is useful for the synthesis of transition metal complexes which play important role in biological systems [11]. Polydentate ligand complexes with an $N_2O_2$, $S_2O_2$, and $N_2S_2$ donor atoms set can also act as tetradentate chelating ligands for metal cations that produce mononuclear complexes. The structures of the ligands are given in Scheme 1. Ligand $L^3$ was found to

**Scheme 1** Structural representation of the ligands

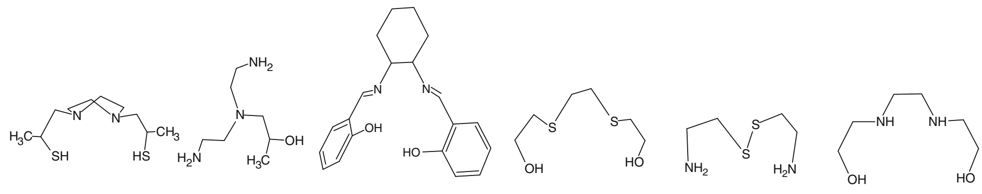


L[1] L[2] L[3] L[4] L[5] L[6]

form 1:1 adduct with Pt(II) [12]. In this article, we report the synthesis, spectroscopic characterization, and thermal stabilities of the Pt(II) complexes of some tri and tetradentate ligands.

## Experimental

All chemicals (include, $L^4$, $L^5$, and $L^6$ ligands) were obtained from commercial suppliers and used as received. All the reactions were carried out at argon saturated solutions in dark environment. The FTIR spectrum of the ligands and complexes were recorded on a Spectrum BX-II Perkin-Elmer spectrophotometer on a KBr pellet. Agilent 8453 Diode Array Spectrophotometer was used for electronic spectra. Elemental analyses were performed on a LECO, CHNO organic element analyzer. Thermogravimetric analysis (TGA) was performed on a Perkin-Elmer Diamond TG/DTA with a heating rate of 10 °C $min^{-1}$ under nitrogen flow (200 mL $min^{-1}$). The residues of thermal decomposition were characterized by a powder X-ray diffractometer (D2 Phaser with Lynxeye). NMR spectra ($^1$H and $^{13}$C) were recorded with a Varian 300 MHz spectrometer. The magnetic susceptibility was measured for the solid samples at room temperature using a Sherwood magnetic susceptibility balance. X-ray structure was solved with a Riqaku RAXIS RAPID imaging diffractometer.

### Synthesis

*Synthesis of 1,1′-piperazine-1,4-diyldipropane-2-thiol ($L^1$)*

Piperazine (1.00 g, 11.60 mmol) was dissolved in 25 mL argon saturated toluene. Propylene sulfide (2.60 g, 34.80 mmol) was dissolved in 10 mL toluene, and this solution was added to piperazine solution. The resulting solution was stirred on magnetic stirrer and heated to 105 °C for 36 h. Subsequently, the solution was allowed to cool to room temperature and product checked for the purity with thin layer chromatography. The product was dissolved in methanol and left for the crystallization. A few days later, colorless crystal was precipitated and dried under vacuum.

Yield: 75%, 2.04 g. Found (%) C, 51.3; H, 9.6; N, 11.8. Calc. for $C_{10}H_{22}N_2S_2$,C, 51.2; H, 9.5; N, 11.9. FT-IR ($cm^{-1}$, KBr): 2919–2807 $\nu$(C–H, aliphatic), 1374 $\nu$(C–N), 2545 $\nu$(S–H). $^1$H-NMR ($\delta$, ppm, $CD_3OH$): 3.09 (N–C–H, aliphatic, triplet), 2.52 (singlet), 2.34 (4H, multiplet), 1.26, 1.24 ($-CH_3$, SH, singlet), $^{13}$C-NMR ($\delta$, ppm, $CD_3OH$): 67.52, 53.03, 31.91, 21.43 (aliphatic). Mass (GC/MS EI): *m/z* 235.02 $[M]^+$.

*Synthesis of (2S)-1-[bis(2-aminoethyl)amino] propan-2-ol ($L^2$)*

Diethylenetriamine (3.09 mL, 30 mmol) 50 mL was dissolved in methanol. (1.50 mL, 30 mmol) propylene oxide was dissolved in argon saturated methanol, and this solution was added to amine solution on magnetic stirrer for 24 h. Solvent volume was reduced at rotary evaporator and left for crystallization. Oily product was obtained, and purity of the product was checked with thin layer chromatography.

Yield: 76%, 3.68 g, Found (%) C, 51.1; H, 11.8; N, 25.9. Calc. for $C_7H_{19}N_3O$,C, 51.1; H,11.9; N, 26.1. FT-IR (KBr $cm^{-1}$): 3304–3291 $\nu$(N–H, OH), 2926–2872 $\nu$(C–H, aliphatic), $^1$H-NMR ($\delta$, ppm, $CDCl_3$): 7.01, 6.71 (C–H, aromatic, singlet), 3.77 (triplet), 3.25 (2H, triplet), 2.54 (2H, triplet), 2.27 (triplet), 2.11(singlet), 1.91 (multiplet), 1.63 (multiplet).$^{13}$C-NMR ($\delta$, ppm, $CD_3OH$): 65.90, 56.85, 51.54, 40.70, 20.55 (aliphatic). Mass. (GC/MS EI): *m/z* 162.30 $[M]^+$.

*Synthesis of 2-{(E)-[((1R,2S)-2-{[(1Z)-(2-hydroxyphenyl)methylene]amino}cyclohexyl) imino] methyl} phenol ($L^3$)*

(2.28 g, 20 mmol) cyclohexane-1,2-diamine and (4.88 g, 40 mmol) 2-hydroxy benzaldehyde dissolved in 50 mL methanol separately. These solutions then were mixed on magnetic stirrer and were stirred upon heating for 1 h at 50° C. Hot solution was filtered and then left for crystallization. A few days later, some crystals were obtained. They were dissolved in hot ethanol and left for crystallization. Crystals were checked with microscope, and their structures were solved with X-ray crystallography.

**Scheme 2** Proposed structures of the Pt(II) complexes

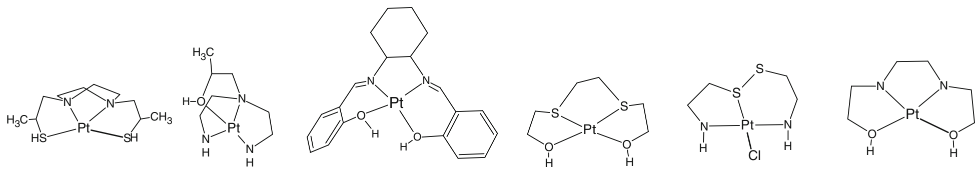

PtL[1] PtL[2] PtL[3] PtL[4] PtL[5] PtL[6]

Yield: 74%, 4.80 g. Found (%) C, 74.3; H, 6.8; N, 8.8. Calc. for $C_{20}H_{22}N_2O_2$,C, 74.5; H, 6.9; N, 8.7. FT-IR ($cm^{-1}$, KBr): 3317 *v*(OH, aromatic), 3048, 3013 (aromatic C–H), 2941–2848 *v*(C–H, aliphatic), 1628 *v*(C=N). $^1$H-NMR ($\delta$, ppm, $CDCl_3$): 13.34 (OH singlet), 8.25 (HC=N, singlet), 7.26–6.77 (C–H, aromatic), 3.29 (H, doublet), 1.90 (2H, triplet), 1.73 (2H, triplet), 1.46 (2H, triplet), $^{13}$C-NMR ($\delta$, ppm, $CDCl_3$): 183.22 (CH=N), 164.90(C–OH), 161.14, 132.28, 131.70, 118.82, 116.97 (aromatic), 72.66, 33.33, 24.40 (aliphatic). Mass. (GC/MS, EI): *m/z* 323.18 $M]^+$.

Preparation of the complexes

(1 mmol, 0.4 g) $K_2[PtCl_4]$ was dissolved in 10 mL argon saturated distilled water, and this solution was added to the(1 mmol) ligand solutions which were dissolved in 10 mL methanol. The mixture was left on magnetic stirrer at 65 °C for 5 h. The solutions were filtered, and solid phase and solution were analyzed for the complexes. Solid phase was dissolved in hot water and kept at 0 °C for 24 h. The resulting precipitate was collected by filtration and washed with cold water and methanol. The complexes were purified by Soxhlet extraction using different solvents. The purified complexes were kept in vacuum desiccators over silica. The proposed structures of the complexes are given in Scheme 2.

Crystal structure determination

A yellow single crystal of the *N,N′*-bis(salicylidene)-1, 2-cyclohexanediamine having dimensions 0.45 × 0.40 × 0.25 $mm^3$ was placed on a Riqaku RAXIS RAPID imaging plate area detector with graphite monochromated Mo-K$\alpha$ radiation. The data were collected at $\lambda = 0.71075$ Å at a temperature of 296 K to a maximum $2\theta$ value of 55.0° by the $\omega$-scan mode in the range $3.1° \leq \theta \leq 27.5°$ with a total of 8,774 reflections collected including 8,591 independent ($R_{int} = 0.086$) reflections. The structure was solved by direct methods [13] and expanded using Fourier techniques [14]. The final cycle of full matrix least-squares refinement [1] on F2 was based on 2,851 reflections. Crystal data and refinement results are listed in Table 1. Selected bond

**Table 1** Crystal data and structure refinement for the $C_{20}H_{20}N_2O_2$

| Chemical formula | $C_{20}H_{20}N_2O_2$ |
|---|---|
| Mass/g $mol^{-1}$ | 320.39 |
| Temperature/K | 296 |
| Wavelength/Å | 0.71075 |
| Crystal system | Monoclinic |
| Space group | Cc/#9 |
| Unit cell dimensions | |
| *a*/Å | 15.920 |
| *b*/Å | 11.793; $\beta = 98.31$ |
| *c*/Å | 9.587 |
| Volume/Å$^3$ | 1781 |
| *Z* | 4 |
| Density (calculated)/Mg $m^{-3}$ | 1.195 |
| Absorption coefficient/$cm^{-1}$ | 0.78 |
| *F*(000) | 680.00 |
| Crystal size/$mm^3$ | 0.45 × 0.40 × 0.25 |
| Range for data collection/$\theta$ (°) | 3.1–27.5 |
| Limiting indices/*h*,*k*,*l* ranges | $-20 \leq 20, -15 \leq 15, -11 \leq 12$ |
| Reflections collected | 8,774 |
| Independent reflections | 8,591/$R_{int} = 0.086$ |
| Refinement method | Full matrix least-squares on $F^2$ |
| Data/restraints/parameters | 4,574/2/281 |
| Goodness of Fit on $F^2$ | 1.025 |
| Final *R* indices/$I > 3\sigma(I)$ | $R_1 = 0.053$, $wR_2 = 0.084$ |
| *R* indices/all data | $R_1 = 0.064$, $wR_2 = 0.092$ |

length and bond distances are given in Table 2. Data collection and processing were performed using crystallographic software package [15, 16]. The final agreement factor values are $R_1 = 0.053$, $wR_2 = 0.084$ $[I > 3.0\sigma(I)]$. Molecular structure of the $L^3$ is given in Fig. 1, and unit cell is given in Fig. 2.

Thermal studies

Thermal decomposition behaviors of the complexes have been studied under dynamic nitrogen atmosphere at a heating rate 10 °C $min^{-1}$. 7–10 mg dried samples on a ceramic sample holder were used for the thermal analysis. Thermal decompositions were recorded in the temperature range 10–1000 °C.

[1] Least-squares function minimized: $w(F_o^2 - F_c^2)^2$, where $w$ = Least-Squares mass.

**Table 2** Selected bond lengths (Å) and angles (°) for the $C_{20}H_{20}N_2O_2$

| | | | |
|---|---|---|---|
| N1–C8 | 1.474 | N2–C13 | 1.481 |
| N1–C7 | 1.261 | N2–C14 | 1.265 |
| C6–C7 | 1.450 | C14–C15 | 1.458 |
| C1–O1 | 1.367 | C20–O2 | 1.347 |
| Dihedral angles | | | |
| N1–C7–C6 | 122.5 | N2–C14–C15 | 122.8 |
| O1–C1–C6 | 119.9 | O2–C20–C15 | 121.4 |

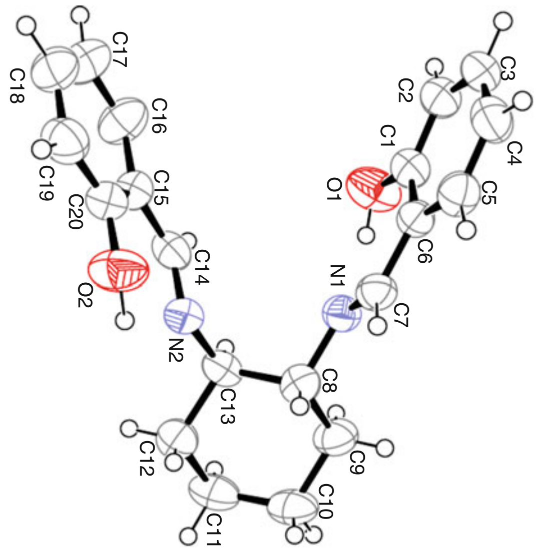


**Fig. 1** Crystal structure of the $L^3$ ligand with atomic numbers

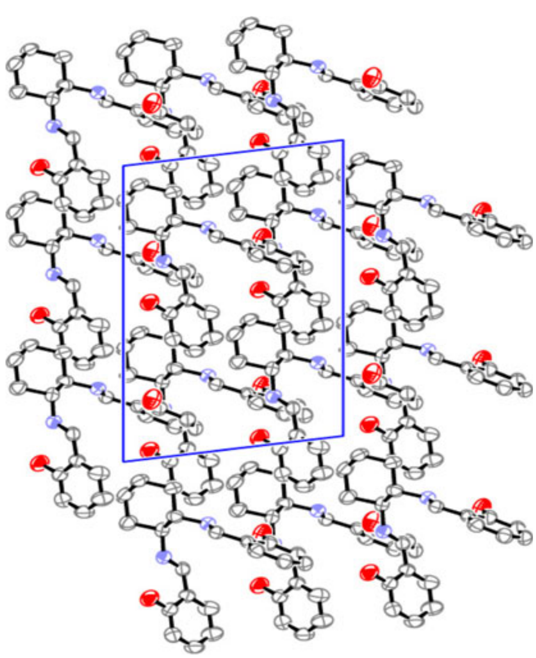

**Fig. 2** Crystal packing of the $L^3$ ligand

## Results and discussion

### Compound characterization

The structure of the ligands was characterized by FTIR, EI Mass, $^1H$ and $^{13}C$ NMR, and elemental analysis. The structure of the $L^3$ ligands was characterized by X-ray single crystal diffractometer. The characterization of the complexes was performed by FTIR, elemental analysis, magnetic measurements, and thermal studies.

**Table 3** Selected FTIR data of the ligands and complexes/cm$^{-1}$

| Compounds | υ/C=N | υ/C–N | υ/C–O | υ/S–H | υ/N–H | υ/O–H |
|---|---|---|---|---|---|---|
| $L^1$ | – | 1374 | – | 2546 | – | 3381 |
| $PtL^1$ | – | 1378 | – | 2340 | – | 3400 |
| $L^2$ | – | 1463 | 1319 | – | 3291 | 3291 |
| $PtL^2$ | – | 1457 | 1374 | – | 3132 | 3435 |
| $L^3$ | 1628 | 1423 | 1279 | – | – | 2659 |
| $PtL^3$ | 1620 | 1449 | 1311 | – | – | 3194, 3268 |
| $L^4$ | – | – | 1343 | – | – | 3291 |
| $PtL^4$ | – | – | 1402 | – | – | 3344 |
| $L^5$ | – | – | – | – | 3155 | – |
| $PtL^5$ | – | – | – | – | 3195 | – |
| $L^6$ | – | 1475 | 1357 | – | 3270 | – |
| $PtL^6$ | – | 1448 | 1365 | – | 3123 | 3336 |

**Table 4** Elemental analyses of the Pt(II) complexes

| Compound | C% | H% | N% | Pt% |
|---|---|---|---|---|
| $[PtL^1]Cl_2{\cdot}2H_2O$ | | | | |
| Calculated | 22.56 | 4.16 | 5.26 | 36.64 |
| Found | 22.68 | 4.02 | 5.12 | 36.77 |
| $[PtL^2]Cl_2$ | | | | |
| Calculated | 19.73 | 4.26 | 9.86 | 45.77 |
| Found | 20.02 | 4.1 | 9.66 | 45.58 |
| $[PtL^3]Cl_2{\cdot}H_2O$ | | | | |
| Calculated | 39.68 | 3.83 | 4.63 | 32.22 |
| Found | 40.11 | 3.68 | 4.55 | 32.33 |
| $[PtL^4]Cl_2$ | | | | |
| Calculated | 16.08 | 3.15 | | 43.52 |
| Found | 16.33 | 2.96 | | 43.27 |
| $[PtL^5]Cl_2{\cdot}0.5H_2O$ | | | | |
| Calculated | 11.54 | 2.42 | 6.73 | 46.87 |
| Found | 11.68 | 2.22 | 6.65 | 47.12 |
| $[PtL^6]Cl_2$ | | | | |
| Calculated | 17.4 | 3.89 | 6.76 | 47.4 |
| Found | 17.35 | 3.77 | 6.58 | 47.33 |

## FTIR spectra of the complexes

The most relevant IR peaks of the ligand were compared, and the most relevant peaks are given in Table 3. The O–H stretching of the free ligand, $L^3$ was expected in the range 3300–3700 $cm^{-1}$ region, but this peak was shifted to 2659 or lower region due to the strong inner molecular hydrogen bonding with the imine nitrogen [17]. The N–H stretching vibration is observed in the 3100–3250 $cm^{-1}$. The υC=N band is observed at 1628 $cm^{-1}$ in free ligand, and this band is shifted to 1620 $cm^{-1}$ in the Pt(II) complex. The S–H stretching was observed in $L^1$ at 2546 $cm^{-1}$. The υC–O bands are generally observed in the region of 1270–1330 $cm^{-1}$ for free ligands and 1305–1330 $cm^{-1}$ for complexes. The shift of υC=N of the free ligands to lower values as well as of υC–O to higher values in the corresponding complexes was taken as evidence for the coordination of both imino and hydroxyl group. This was supported by the results of elemental analysis of the complexes (Table 4).

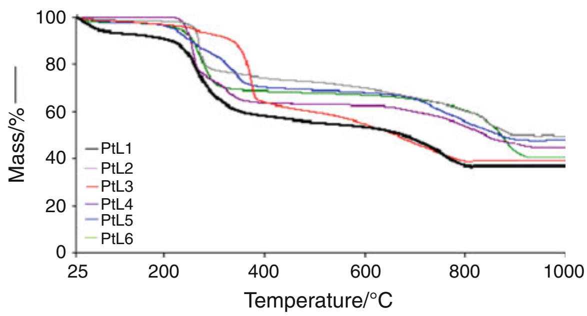


**Fig. 3** TG curves of the Pt(II) complexes in nitrogen atmosphere with heating rate/10 °C $min^{-1}$. Sample holder: silica, sample mass: 7–10 mg

## Thermal analysis

TG curve of the complexes show two- and three-step decompositions. $PtL^1$, $PtL^2$, and $PtL^3$ show three-step decompositions, while $PtL^4$, $PtL^5$, and $PtL^6$ show two-step decompositions. The thermal decomposition of the Pt(II) complexes exhibit several thermal events. The TG curve of the complexes is given in Fig. 3. The first mass loss is observed in the temperature range of 10–200 °C which corresponds to the loss of water molecules in the structures. The second mass loss is observed from 200 to 400 °C which corresponds to the fragment of coordinated ligand in

**Table 5** Thermo analytical results for the Pt(II) complexes

| Compound | TG range/°C | $DTG_{max}$ /°C | Removed group | Mass loss Found | Mass loss Calc./% | Total mass% loss | Residue |
|---|---|---|---|---|---|---|---|
| $[PtL^1]Cl_2 \cdot 2H_2O$ | | | | | | | |
| | 10–145 | 73 | $2H_20$ | 6.8 | 6.7 | | |
| | 150–640 | 263 | $C_{10}H_{22}N_2S_2$ | 43.52 | 43.73 | | |
| | 650–825 | 772 | 2Cl | 13.22 | 13.24 | 63.54 | PtO |
| $[PtL^2]Cl_2 \cdot H_2O$ | | | | | | | |
| | 10–290 | 271 | $C_3H_8O$ | 12.81 | 12.82 | | |
| | 300–890 | 839 | 2Cl,$C_4H_{12}N_3$ | 37.12 | 37.19 | 50.01 | PtO |
| $[PtL^3]Cl_2 \cdot H_2O$ | | | | | | | |
| | 10–235 | 262 | $H_2O$ | 2.76 | 2.77 | | |
| | 240–400 | 367 | $C_{13}H_{15}NO$ | 32.12 | 33.14 | | |
| | 410–800 | 677 | 2Cl,$C_7H_7NO$ | 29.04 | 31.63 | 64.28 | PtO |
| $[PtL^4]Cl_2$ | | | | | | | |
| | 10–290 | 264 | $C_4H_{10}O_2$ | 20.48 | 20.51 | | |
| | 300–380 | 325 | 2Cl | 15.76 | 15.83 | | |
| | 390–950 | 833 | $C_2H_4S_2$ | 20.1 | 20.07 | 56.34 | PtO |
| $[PtL^5]Cl_2$ | | | | | | | |
| | 10–200 | 72 | $0.5H_2O$ | 2.2 | 2.12 | | |
| | 210–400 | 342 | 2Cl, $C_2H_6N$ | 26.78 | 26.93 | | |
| | 410–940 | 736 | $C_2H_6NS_2$ | 23.74 | 24.27 | 52.72 | PtO |
| $[PtL^6]Cl_2$ | | | | | | | |
| | 10–350 | 284 | 2Cl, $C_4H_4N_2$ | 31.41 | 31.62 | | |
| | 360–940 | 917 | 2(C2H4OH) | 22.38 | 21.72 | 54.12 | PtO |

the structure. In all the complexes, rapid mass loss observed around 300 °C, indicative of decomposition of the coordinated ligand. The second mass loss is observed from 700 to 900 °C which corresponds to the second fragment of the ligand. Finally, the plateau obtained after heating the complex above 900 °C corresponds to the formation of stable PtO. Metal content calculated from these residues for Pt(II) complexes are in good agreement with the metal analysis. The mass loss, temperature ranges, and the description of the thermal events observed in this study are summarized in Table 5. After dehydration, $PtL^3$ complex presents the higher decomposition temperatures for the series of the compounds. The order for the thermal stability is found as $PtL^3 > PtL^5 > PtL^2 > PtL^6 > PtL^4 > PtL^1$. This stability order should be related with the structure of the ligands. Thermal decomposition of the complexes is two steps after dehydration. Chloride behaves as counter ion at all complexes. The structure of aliphatic mixed donor ligands shows low thermal stability when compared with aromatic ligand. The decomposition reaction of aromatic Pt(II) begins with the cleavage of M–N bond. As basicity of the ligand increases, thermal stability also increases. Thermal stability of the complexes depends on the interactions of donor atom and Pt(II). The crystal water plays a significant role on the thermal stability. The presence of the water keeps the structure less flexible with inner and inter hydrogen bonds, so that the complex structures are more tightly combined each other and thermal stability is affected according to the strength of the hydrogen bonds.

## Conclusions

The large thermal stability of $PtL^3$ can be attributed to a decrease steric constraint imposed on ligand by the presence of the two 6-membered ring and one crystal water in the square planer configuration. The second stable complex is the $PtL^5$ which has also one 6-membered ring in the structure. Using the hard soft-acid base theory it is suggested that sulfur containing low molecular weight molecules can be specifically targeted to complexation using soft metal ions such as Pt(II). These results show that a series of linked 5-membered rings become sterically constrained on coordination to a metal. The replacement of a 5-membered ring with 6-membered ring by a 6-membered ring can reduce the steric constraints and lead to an increase in thermal stability.

**Acknowledgements** The authors wish to thank the Scientific and Technological Research Council of Turkey (TUBITAK) for financial support (project no: 104T389) and BAP. Scientific Research Project of COMU.

## References

1. Chantarasiri N, Tuntulani T, Tongraung R, Seangprasertkit-Magee R, Wannarong W. New metal-containing epoxy polymers from diglycidyl ether of bisphenol A and tetradentate Schiff base metal complexes. Eur Polym J. 2000;36:695–702. doi:10.16/50014-3057(99)00127-5.
2. Pignatello R, Panico A, Mazzone P, Pinizzotto MR. Garozzo APM: Fumeri Schiff bases of *N*-hydroxy-*N*′-aminoguanidines as antiviral, antibacterial and anticancer agents. Eur J Med Chem. 1994;29:781–5. doi:10.1016/0223-5434(94)90137-6.
3. Guofa L, Tongshun S, Yongnian Z. Infrared and Raman spectra of complexes about rare earth nitrate with Schiff base from *o*-vanillin and 1-naphthylamine. J Mol Struct. 1997;412:75–81. doi:10.1016/S0022-2860(97)00026-4.
4. Albertin G, Bordignon E, Orio AA. Five-coordinate copper(II) complexes. Synthesis and properties of $[Cu(tren)L]^{2+}$ cations. Inorg Chem. 1975;14:1411–3. doi:10.1021/ic50148a042.
5. Raman N, Kulondaisamy A, Thangarja C, Jeyasubramanian. Redox and antimicrobial studies of transition metal(II) tetradentate ligands. Trans Met Chem. 2003;28:29–36. doi:10.1023/A:1022544126607.
6. Raman N, Kulandaisamy A, Jeyasubramanian K. Synthesis, spectroscopic characterization, redox, and biological screening studies of some Schiff base transition metal(II) complexes derived from salicylidene-4-aminoantipyrine and 2-aminophenol/2-aminothio phenol. Synth React Inorg Met Org Chem. 2001;31:1249–70. doi:10.1081/SIM-100106862.
7. Tarafder MTH, Ali MA, Sarvanan N, Weng WY, Umar Tsafe N, Crouse KA. Coordination chemistry and biological activity of two tridentate ONS and NNS Schiff bases derived from *S*-benzyldithiocarbazate. Trans Met Chem. 2000;25:295–8. doi:10.1023/A:1007044910814.
8. Collman J, Hegadus LS. Principals and application of organotransition metal chemistry. Mill Valley: University Science Books; 1980.
9. Zhao J, Zhao B, Liu J, Xu W, Wang Z. Spectroscopy study on the photochromism of Schiff bases *N*,*N*-bis(salicylidene)-1,2-diaminoethane and *N*,*N*-bis(salicylidene)-1,6-hexanediamine. Spectrochim Acta. 2001;57A:149–54. doi:10.1016/S1386-1425(00)00353-X.
10. Zgierski MZ, Grabowska A. Theoretical approach to photochromism of aromatic Schiff bases: a minimal chromophore salicylidene methylamine. J Chem Phys. 2000;113:7845–53. doi:10.1063/1.1316038.
11. Kaim W, Schwederski B. Bioinorganic chemistry: inorganic elements in the chemistry of life. New York: Wiley; 1996.
12. Szlyk E, Barwiolek M, Kruszynki R, Bartczak T. Synthesis and spectroscopic studies of the optically active copper(II), cobalt(II) and nickel(II) complexes with Schiff bases *N*,*N*′-(1*R*, 2*R*)(−)-1,2-cyclohexylenebis(3-methoxybenzylideneiminato), *N*,*N*′-(1*R*, 2*R*)(−)-1,2-cyclohexylenebis(5-methoxybenzylideneiminato) and X-ray diffraction structure of the [Cu(II)(1*R*, 2*R*)(−)chxn-bis(5-methylbenzylideneiminato)2]. Inorg Chim Acta. 2005;358:3642–52. doi:10.1016/j.ica2005.06.032.
13. Altomare A, Cascarano G, Giacovazzo C, Guagliardi A, Burla M, Polidori G, Camalli MA. Program for automatic solution of crystal structures by direct methods. J Appl Cryst. 1994;27:435. doi:10.1107/S0022188989400021X.
14. Beurskens PT, Admiraal G, Beurskens G, Bosman WP, de Gelder R, Israel R, Smits JMM. The DIRDIF-99 program system, technical report of the crystallography laboratory. The Netherlands: University of Nijmegen; 1999.
15. Crystal Structure 3.6.0: Crystal Structure Analysis Package, Rigaku and Rigaku/MSC (2000-2004). 9009 New Trails Dr. The Woodlands TX 77381 USA.

16. Watkin DJ, Prout CK, Carruthers JR, Betteridge PW. CRYSTALS Issue 10. Chemical crystallography laboratory. Oxford: University of Oxford; 1996.
17. Felicio RC, Cavalherio ET, Dockal ER. Preparation, characterization and thermo gravimetric studies of [*N*,*N*-*cis*-1,2-cyclohexylene bis(salicylideneaminato)] cobalt(II) and [*N*,*N*-(9)-*trans*-1,2-cyclohexylene bis(salicylideneaminato)] cobalt(II). Polyhedron. 2001; 20:261–8. doi:10.1016/S0277-5387(00)00620-3.